

# The mechanism of sound generation in the interaction between a shock wave and two counter-rotating vortices

Shuhai Zhang,<sup>1,a)</sup> Shufen Jiang,<sup>2</sup> Yong-Tao Zhang,<sup>3,b)</sup> and Chi-Wang Shu<sup>4,c)</sup>

<sup>1</sup>State Key Laboratory of Aerodynamics, China Aerodynamics Research and Development Center, Mianyang, Sichuan 621000, China

<sup>2</sup>China Aerodynamics Research and Development Center, Mianyang, Sichuan 621000, China

<sup>3</sup>Department of Mathematics, University of Notre Dame, Notre Dame, Indiana 46556, USA

<sup>4</sup>Division of Applied Mathematics, Brown University, Providence, Rhode Island 02912, USA

(Received 21 April 2008; accepted 19 May 2009; published online 15 July 2009)

The interaction between a shock wave and two counter-rotating vortices is simulated systematically through solving the two-dimensional, unsteady, compressible Navier–Stokes equations using a fifth order weighted essentially nonoscillatory finite difference scheme. The main purpose of this study is to reveal the mechanism of sound generation in the interaction between a shock wave and two counter-rotating vortices. It is found that there are two regimes of sound generation in this interaction. The first regime corresponds to the shock interaction with two isolated vortices, in which the sound wave generated by the interaction between the shock wave and two counter-rotating vortices equals to the linear combination of the sound waves generated by the interactions between the same shock wave and each vortex. The second regime corresponds to the shock interaction with a coupled vortex pair, in which the sound wave comes from two processes. One is the vortex coupling, and the second is the interaction between the shock wave and the coupled vortex pair. © 2009 American Institute of Physics. [DOI: 10.1063/1.3176473]

## I. INTRODUCTION

Shock waves and vortices are two basic elements of compressible flow. The interaction between them is a common phenomenon and is very important in many applications such as supersonic mixing layers, supersonic jets, and combustion instability. In particular, because a number of shock waves and vortices coexist in the complicated supersonic turbulence flow, the interaction of a shock wave and vortices can be seen as a simplified model of shock turbulence interaction, which is one of the major sources of noise and has received increasing attention.

The interaction of a shock wave and a single vortex is one of the most simplified models of shock turbulence interaction and has been extensively studied through experiment,<sup>1–3</sup> theoretical analysis,<sup>4–7</sup> and direct numerical simulation.<sup>8–11</sup> The nature of the sounds generated by this interaction has been clarified to a significant extent. These studies have revealed several basic mechanisms of sound generation in shock turbulence interaction. A brief summary is given by Inoue and Hattori<sup>12</sup> and Zhang *et al.*<sup>13</sup>

However, there is a significant difference between shock single vortex interaction and shock turbulence interaction. Since the mechanism of sound generation in shock turbulence interaction is far from being fully understood, it is necessary to study more complicated models than that for shock single vortex interaction. The interaction of a shock wave and a vortex pair is more complicated than the interaction of a shock wave and a single vortex. It has closer

relationship to shock turbulence interaction than shock single vortex interaction does. For instance, there are a street of vortices in a shear layer and wake flow. Coupling and merging of two vortices are two key phenomena in these vortices dominated flow. There are many similar features in shock vortex pair interaction and shock shear layer interaction which plays an important role in supersonic jet noise.<sup>14–16</sup> Compared to the shock single vortex interaction, there are fewer studies on the interaction of a shock and a vortex pair. Inoue *et al.*<sup>12,17</sup> and Pirozzoli *et al.*<sup>18</sup> studied the interaction of a shock and two vortices in tandem and in parallel patterns. Zhang *et al.*<sup>19</sup> studied the interaction of a shock wave and two vortices with arbitrary position to the shock wave. The pattern of the flow structure, especially the shock structure, is classified. Numerical studies show that it contains new mechanisms of sound generation not found in shock single vortex interaction.

This paper is an extension of our previous work in Ref. 19. Our purpose is to study the mechanism of sound generation in the interaction between a shock wave and two counter-rotating vortices through simulating the two-dimensional Navier–Stokes equation using a fifth order weighted essentially nonoscillatory (WENO) scheme.<sup>20</sup> The effect of the strength of the vortices and the geometry parameters are studied systematically. Our study shows that there are two different regimes of sound generation in the shock interaction with two counter-rotating vortices. One is the shock interaction with two isolated vortices, and the other is the shock interaction with a coupled vortex pair.

This paper is organized as follows. In Sec. II, the numerical method and the physical model are introduced. In Sec. III, we present our simulation results and provide a de-

<sup>a)</sup>Electronic mail: zhang\_shuhai@tom.com.

<sup>b)</sup>Electronic mail: yzhang10@nd.edu.

<sup>c)</sup>Electronic mail: shu@dam.brown.edu.

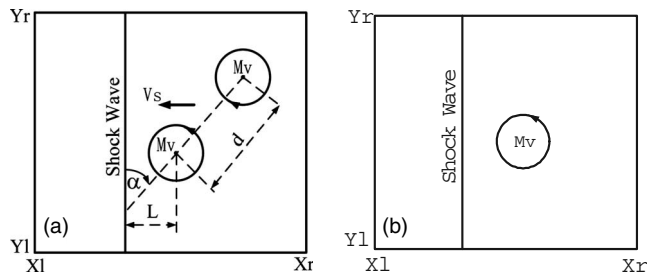


FIG. 1. Schematic diagram of the flow model. (a) shock interaction with two counter-rotating vortices; (b) shock interaction with a single vortex.

tailed discussion for the sound generation. Section IV contains our concluding remarks.

## II. THE PHYSICAL MODEL

The numerical method is the same as that by Zhang *et al.*<sup>13,19</sup> Two-dimensional unsteady compressible Navier–Stokes equations are simulated by the fifth order WENO finite difference scheme developed by Jiang and Shu.<sup>20</sup> We refer to Ref. 13 for more details.

Figure 1 is the schematic diagram of the flow model. Figure 1(a) is the schematic diagram of the interaction between a shock wave and two counter-rotating vortices.  $L$  is the initial distance between the first vortex and the incident shock wave, and  $d$  is the initial separation distance of the two vortices. These are the key parameters to study the mechanism of sound generation in shock vortex pair interaction.  $\alpha$  is the angle between the incident shock wave and the vortex pair.  $M_v$  is the strength of the vortices. To reveal the different mechanisms of sound generation between the shock interaction with two counter-rotating vortices and the shock interaction with a single vortex, we also simulate the interactions of the shock wave and each single vortex, which is schematically shown in Fig. 1(b). Figure 1(b) corresponds to the interaction of the shock wave and the first (lower) vortex of the vortex pair. The interaction between the shock wave and the second (upper) vortex has the same schematic pattern except for the position and the rotating direction of the vortex. The computational domain is prescribed to be rectangular  $x_l < x < x_r$ ,  $y_l < y < y_r$ . The shock wave of Mach number  $M_s = 1.2$  is set to be stationary at  $x = 0$  in the computation. The vortex pair or the isolated vortex moves toward the shock at the speed of the shock wave,  $V_s$ .

The initial value of the vortex parameters<sup>12,13</sup> in the shock interaction with a single vortex is set as follows. The tangential velocity

$$u_\theta(r) = M_v r e^{(1-r^2)/2},$$

radial velocity

$$u_r = 0,$$

pressure

$$p(r) = \frac{1}{\gamma} \left[ 1 - \frac{\gamma-1}{2} M_v^2 e^{1-r^2} \right]^{\gamma/(\gamma-1)},$$

and density

TABLE I. Parameters used in the simulations of shock interaction with two counter-rotating vortices and different regimes each simulation falls into.

Regime	$M_v$	$d$	$L$	$\alpha$ (deg)
$R_1$	0.05	4	4	0
				45
				90
	0.25	4	4	0
				45
				90
$R_2(a)$	0.25	6	4	0
				45
				90
	0.50	4	...	0
				0.80
				0.80
$R_2(b)$	0.80	4	45	0
	$R_2(c)$	0.25	4	4
0.25		4	20	45
0.80		4	20	45
0.80		4	50	45

$$\rho(r) = \left[ 1 - \frac{\gamma-1}{2} M_v^2 e^{1-r^2} \right]^{1/(\gamma-1)},$$

where  $r = \sqrt{(x-x_v)^2 + (y-y_v)^2}$ .  $(x_v, y_v)$  is the center of the initial vortex.  $\gamma = 1.4$  is the ratio of specific heats. The initial flow field for the case of the vortex pair is prescribed by the superposition of the flow field produced by each single vortex. The initial location of the first vortex is prescribed to be  $x_d = L, y_d = -(d/2)\cos(\alpha)$  and that of the second vortex to be  $x_u = L + d \sin(\alpha), y_u = (d/2)\cos(\alpha)$ .

## III. SIMULATION RESULTS

There are two different regimes of sound generation in the shock interaction with two counter-rotating vortices. The first regime corresponds to the shock interaction with two isolated vortices. When the vortices are weak or the separation distance between the two vortices is large, the sound wave generated by the interaction between the shock wave and the vortex pair equals to the linear combination of the sound waves generated by the interactions between the same shock wave and each single vortex. The second regime corresponds to the coupling effect of the two vortices. During the interaction of the shock wave and the vortex pair, the two vortices undergo a coupling process which generates sound waves.

In Table I, we list the parameters used in our simulation for the interaction between a shock wave and two counter-rotating vortices and the regimes each simulation falls into.  $R_1$  refers to the regime of the shock interaction with two isolated vortices.  $R_2(a)$  represents the regime of the free evolution of the coupling process of the two counter-rotating vortices which generates two vortex dipoles (with no shocks involved).  $R_2(b)$  represents the regime for the vortex coupling in regime  $R_2(a)$  followed by the subsequent interaction

between a shock wave and these two vortex dipoles. In this case,  $L$  represents the distance between the incident shock wave and the vortex dipole resulting from the coupling effect of two counter-rotating vortices of strength  $M_v$ .  $R_2(c)$  represents the interaction of the shock wave and a vortex pair that is simultaneously going through the coupling process. In each case falling into the regime  $R_1$ , we also perform simulations for the interactions between the same shock and each single vortex.

### A. Shock interaction with two isolated vortices

In the shock interaction with two isolated vortices, the sound generated by the shock interaction with the vortex pair equals to the linear combination of the two interactions between the same shock wave and each single vortex. This regime, denoted by  $R_1$  in Table I, corresponds to the interaction between a shock wave and a weak vortex pair or a vortex pair with a large separation distance. With a given strength of the vortex pair, the separation distance  $d$  is the key parameter that influences the realization of this regime.

In our study, we simulate and compare the sound wave generated by the interaction between a shock wave and two counter-rotating vortices and the linear combination of sound waves generated by the two interactions between the same shock wave and each vortex. Figure 2 contains the sound pressure of such a comparison. The Mach number of the shock wave is  $M_s=1.2$ . The strength of the vortices is  $M_v=0.05$ . The initial distance between the shock wave and the vortex pair and the separation distance between the two vortices are both 4. The angles between the vortex pair and the shock wave are  $\alpha=0^\circ$ ,  $45^\circ$ , and  $90^\circ$ , respectively. The left picture contains the contours of the sound pressure and the right one contains the circumferential distribution. This figure shows that, for this set of parameters, the sound pressure generated by the shock interaction with two counter-rotating vortices equals almost exactly to the linear combination of the sound pressures generated by the two interactions between the same shock wave and each vortex. Figure 3 shows the radial distribution of the sound pressure along the direction of the connected line of the two vortex centers. In Fig. 2(c), we can observe that there is a two-cell structure in the second sound wave which was also reported in Ref. 19. As can be seen in Fig. 3, it is the result of the second sound generated by the shock lower vortex interaction merging with the first sound generated by the shock upper vortex interaction.

The strength of the vortex pair  $M_v=0.05$  is very weak. As the strength of the vortices increases, the two vortices undergo a coupling process during the interaction between the shock wave and the vortex pair.

Figure 4 is the sound pressure generated by the interaction of a shock and two counter-rotating vortices and its comparison with the linear combination of the sound waves generated by the two interactions between the same shock and each vortex. The strength of the vortex is now increased to  $M_v=0.25$ . The distance between the two vortices is still  $d=4$ . It is found that the first sound is still the same as that of the linear combination. However, there is some difference in

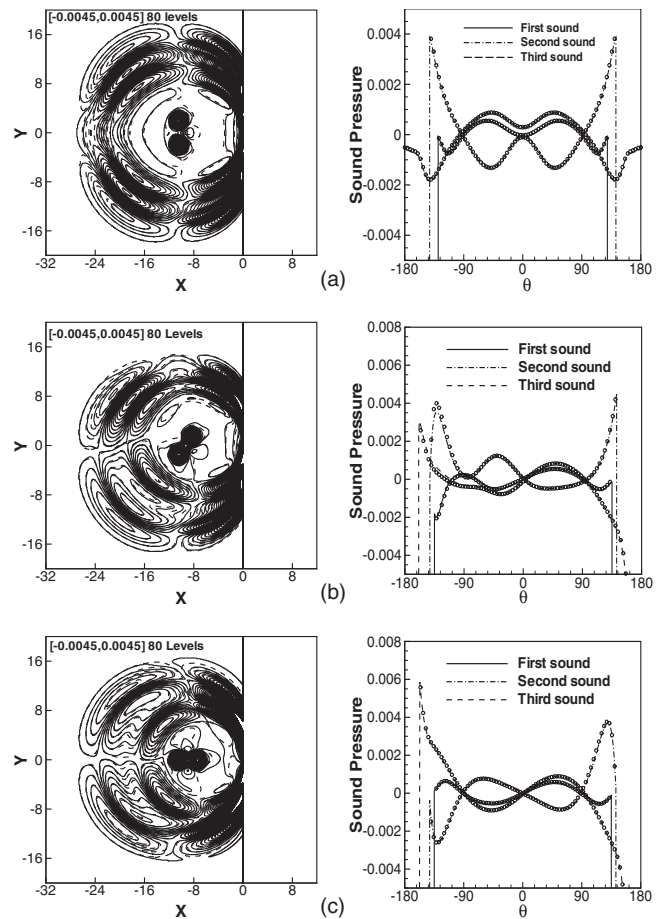


FIG. 2. The comparison of the sound pressure  $[\Delta p=(p-p_s)/p_s]$  generated by the shock interaction with two counter-rotating vortices with the linear combination of the sound waves generated by the two interactions between the same shock and each vortex.  $t=15$ ,  $M_v=0.05$ ,  $M_s=1.2$ ,  $L=4$ , and  $d=4$ . Left: contours of the sound pressure. Solid line: vortex pair; dashed line: linear combination of two isolated vortices. Right: circumferential distribution of sound pressure. Lines: vortex pair; symbols: linear combination of two isolated vortices. (a)  $\alpha=0^\circ$ , (b)  $\alpha=45^\circ$ , (c)  $\alpha=90^\circ$ .

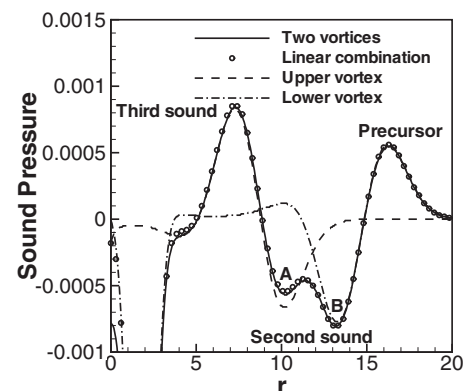


FIG. 3. The sound pressure  $\Delta p=(p-p_s)/p_s$  along the radial direction from the middle of the two vortex centers to the point of the minimum value of the precursor in the negative region at  $t=15$ ,  $M_v=0.05$ ,  $M_s=1.2$ ,  $L=4$ , and  $d=4$ .

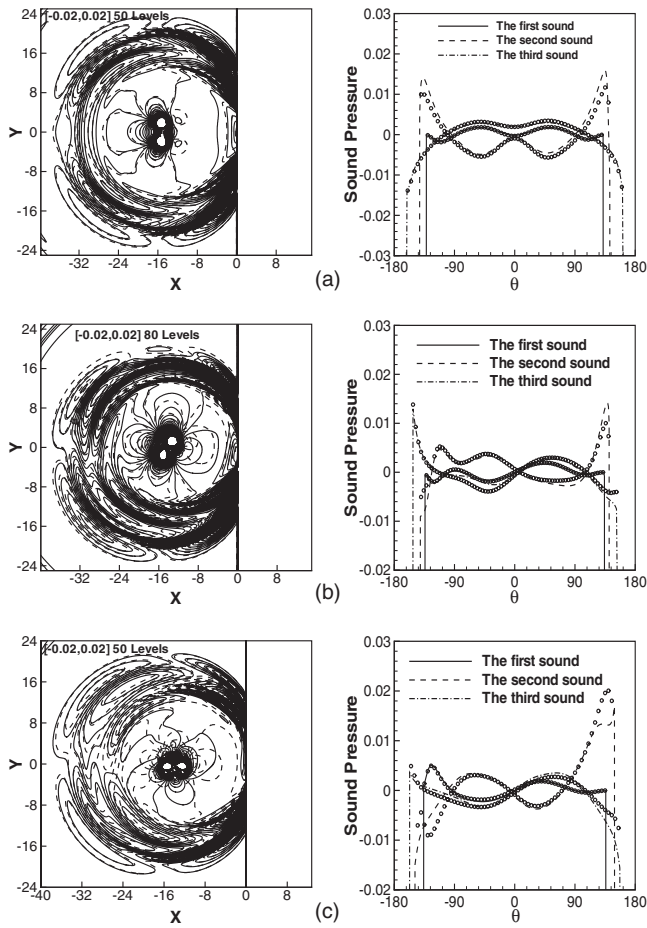


FIG. 4. The comparison of the sound pressure  $[\Delta p = (p - p_s) / p_s]$  generated by the shock interaction with two counter-rotating vortices with the linear combination of the sound waves generated by the two interactions between the same shock and each vortex.  $t = 34$ ,  $M_v = 0.25$ ,  $M_s = 1.2$ ,  $L = 4$ , and  $d = 4$ . Left: contours of the sound pressure. Solid line: vortex pair; dashed line: linear combination of two isolated vortices. Right: circumferential distribution of sound pressure. Lines: vortex pair; symbols: linear combination of two isolated vortices. (a)  $\alpha = 0^\circ$ , (b)  $\alpha = 45^\circ$ , (c)  $\alpha = 90^\circ$ .

the second and the third sound waves. This difference should be the result of the vortex coupling process. If the distance between the two vortices increases, the coupling effect would decrease, and the first regime would be recovered. Figure 5 is the circumferential distribution of the sound pressure for the case of  $M_v = 0.25$  and an increased  $d = 6$ . We can observe that all three sound waves are now within the first regime, similar to the case shown for  $M_v = 0.05$  and  $d = 4$  in Fig. 2.

Numerical experiments indicate that the sound wave generated by the shock vortex pair interaction may fall into the regime of linear combinations of the sound waves generated by the shock interactions with individual vortices. However, the condition for this regime to be realized is different for vortices with different strengths. The stronger the vortices, the larger distance between the two vortices is needed. When the separation is smaller, the coupling effect becomes obvious.

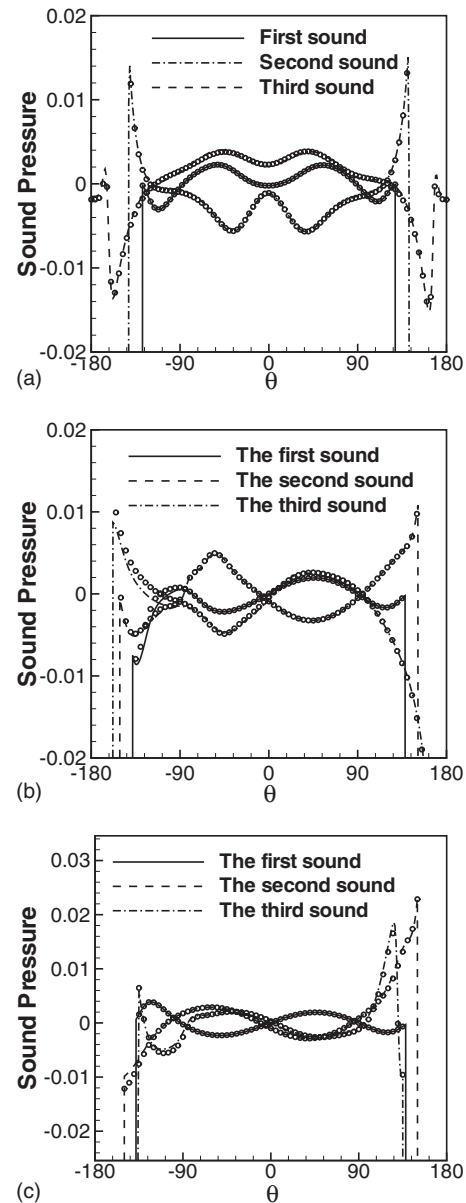


FIG. 5. The comparison of the circumferential distribution of the sound pressure generated by the shock interaction with two counter-rotating vortices with the linear combination of the sound waves generated by the two interactions between the same shock and each vortex.  $t = 34$ ,  $M_v = 0.25$ ,  $M_s = 1.2$ ,  $L = 4$ , and  $d = 6$ . Lines: vortex pair; symbols: linear combination of two isolated vortices. (a)  $\alpha = 0^\circ$ , (b)  $\alpha = 45^\circ$ , (c)  $\alpha = 90^\circ$ .

## B. Shock interaction with coupled vortices

An essential difference between the shock interaction with two counter-rotating vortices and the shock interaction with a single vortex is the possible vortex coupling effect in the former case, which may significantly influence or even dominate in the sound generation process for the shock interaction with two counter-rotating vortices. To better understand this process, we study the sound generation first in the free evolution of the coupling of two vortices, followed by the shock interaction with a vortex dipole (two vortices which have already gone through extensive coupling), and finally the shock interaction with a vortex pair which is simultaneously undergoing the coupling process.



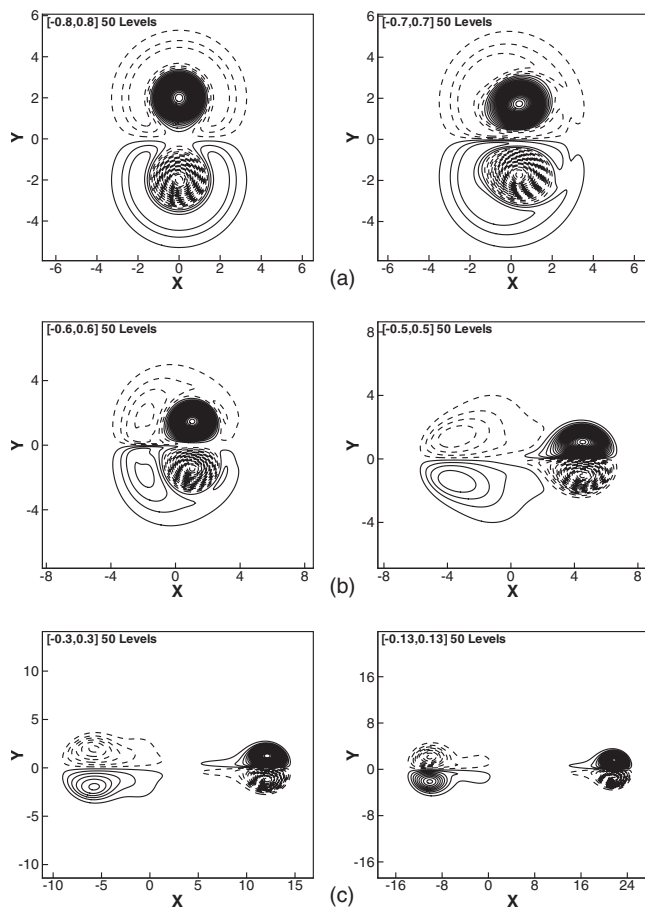


FIG. 6. The evolution of the vorticity field in the vortex coupling of  $M_v = 0.25$ . Solid lines represent the positive vorticity, and dashed lines represent the negative vorticity. (a) left:  $t=0$ ; right:  $t=30$ ; (b) left:  $t=50$ ; right:  $t=100$ ; (c) left:  $t=200$ ; right:  $t=400$ .

### 1. The free evolution of vortex coupling

If two counter-rotating vortices are close enough, they will undergo a movement of vortex coupling, which will result in a new flow structure and generate sound waves.

Figure 6 is the evolution of the vorticity in the vortex coupling process, which is referred to as regime  $R_2(a)$  in Table I. The strength of the vortices is  $M_v = 0.25$ . The lower vortex rotates clockwise and the upper vortex rotates in the opposite direction. The vortices are initially located at the center of the computational domain with a distance  $d=4$ . As can be seen from Fig. 6(a) (left), the isentropic vortex has two layers, the inner layer and the outer layer, in which the sign of vorticity is opposite. In the process of vortex coupling, the vortices undergo a change in shape. The vortex cores are pressed to an approximately elliptical shape from the initially cylindrical shape and they gradually form a vortex dipole with a tail. There is an induced velocity and the vortex dipole is advected to the right. The outer layer is separated from the vortex core and moves toward the symmetry axis. They form a weak vortex dipole which moves to the left. The evolution of the vortex coupling process of this isentropic vortex pair is similar to that of the Taylor-type vortex pair coupling<sup>21</sup> and was observed in the experiment by Schmidt *et al.*<sup>22</sup>

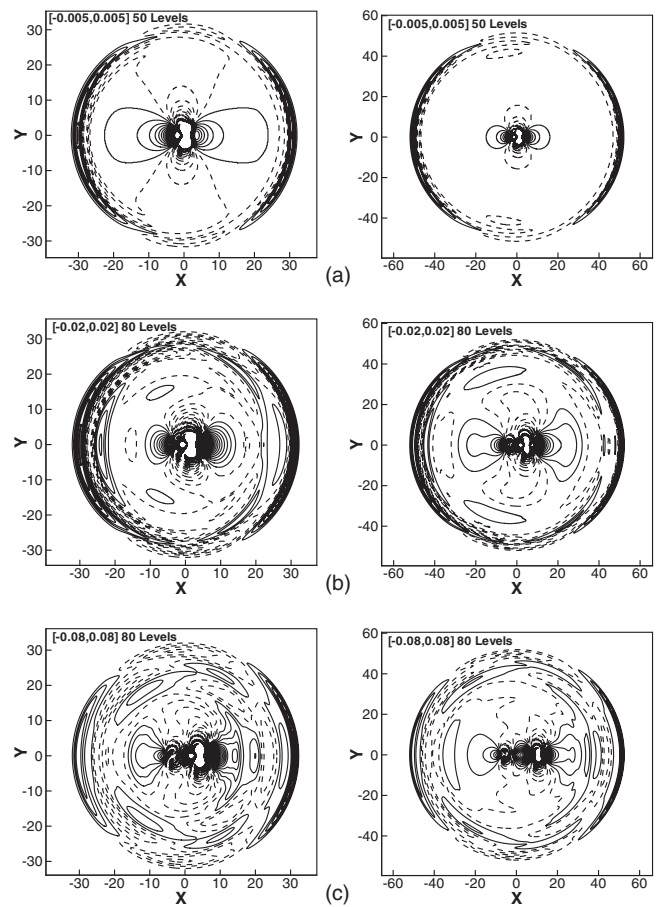


FIG. 7. The contours of the sound pressure  $\Delta p = (p - p_0) / p_0$  in vortex coupling. Left:  $t=30$ . Right:  $t=50$ . Solid lines represent  $\Delta p > 0$ , while dashed lines represent  $\Delta p < 0$ . (a)  $M_v = 0.25$ , (b)  $M_v = 0.5$ , (c)  $M_v = 0.8$ .

Sound waves are generated at the beginning of the vortex coupling. Figure 7 is the sound pressure generated by the vortex coupling for typical strengths of the vortex pair at times  $t=30$  and  $50$ . We can observe that the sound waves have a quadrupolar nature. In the case of weak vortex pair coupling ( $M_v = 0.25$ ), there are only two sound waves. As the vortex becomes stronger, there are more sound waves generated and the sound waves become stronger. Figure 8 is the circumferential and radial (along the symmetric line) distributions of the sound wave. Pirozzoli *et al.*<sup>18</sup> gave the decay law of the first and second sound peaks for  $M_v = 0.25$ .

### 2. Interaction between a shock and a vortex dipole

If the initial distance between the shock wave and two counter-rotating vortices is large enough, the initial vortex pair evolves into two vortex dipoles by the coupling effect as described in Sec. III B 1. The interaction between the shock wave and the vortex pair becomes the interaction of the shock wave and these two vortex dipoles, which is referred to as regime  $R_2(b)$  in Table I. Hence, it is necessary to figure out the characteristic behavior of the sound generation by the shock and vortex dipole interaction.

Figure 9 is the evolution of the sound pressure generated by the interaction of a shock and a vortex dipole. The vortex dipole is the primary one formed by the vortex coupling of

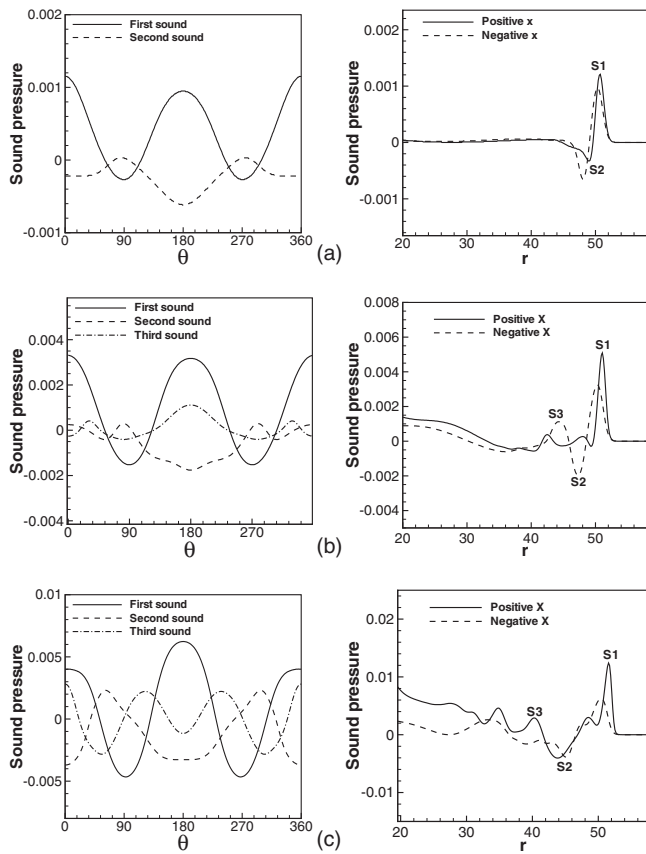


FIG. 8. The circumferential (left) and radial (right) distributions of the sound pressure in vortex coupling at  $t=50$ . (a)  $M_v=0.25$ , (b)  $M_v=0.5$ , (c)  $M_v=0.8$ .

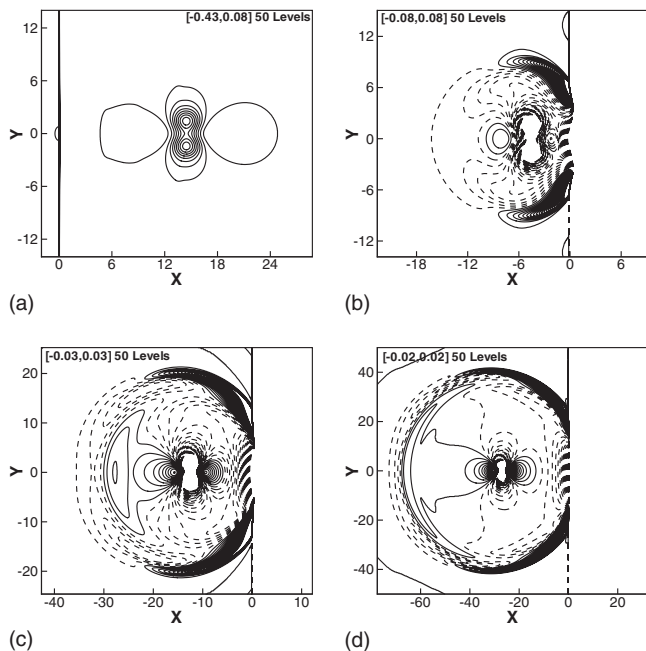


FIG. 9. The contours of the sound pressure  $\Delta p=(p-p_s)/p_s$  by the interaction of a shock wave and a vortex dipole with  $M_v=0.8$ . Solid lines represent  $\Delta p>0$ , while dashed lines represent  $\Delta p<0$ . (a)  $t=30$ , (b)  $t=40$ , (c)  $t=60$ , (d)  $t=80$ .

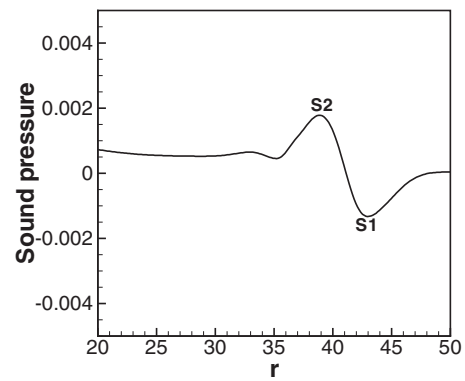


FIG. 10. The radial distribution of the sound pressure of shock vortex dipole interaction with  $M_v=0.8$ .

$M_v=0.8$  when we run to  $t=200$ . The initial distance of the shock wave and the vortex dipole is  $L=45$ . Figure 9(a) shows the case that the tail of the vortex dipole has just reached the shock wave. As the shock wave passes through the vortex dipole, two sound waves are generated. This is quite similar to the sound wave generated by the free evolution of weak vortex coupling. Figure 10 is the distribution of the sound wave along the symmetry line. Compared with the sound wave generated by the vortex coupling given in Fig. 8(c), the sound wave generated by the shock interaction with a vortex dipole is much weaker. The reason is that the vorticity has decayed dramatically when the vortex dipole is formed from the vortex pair.

### 3. Interaction between a shock and a coupling vortex pair

If the distance between the shock wave and the two counter-rotating vortices is not large enough, the two sound generation processes happen at the same time. The sound wave generated by the two different processes, namely, the vortex coupling and the shock vortex interaction, merges together. This scenario is referred to as regime  $R_2(c)$  in Table I. In this case, the distance between the shock wave and the vortex pair is a key parameter of the combined process.

Figure 11 is the sound pressure of  $M_s=1.2$  and  $M_v=0.25$  at  $t=15$ . The initial distance between the shock wave and the

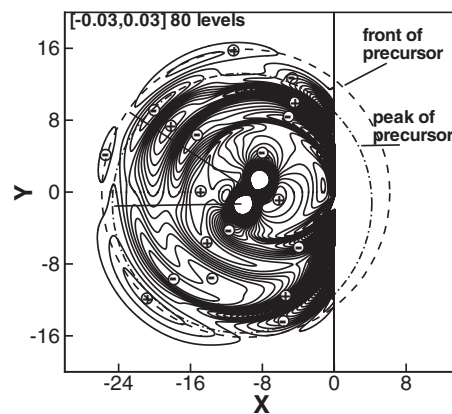


FIG. 11. The sound pressure  $\Delta p=(p-p_s)/p_s$  of the shock interaction with two counter-rotating vortices.  $M_s=1.2$ ,  $M_v=0.25$ ,  $L=d=4$ , and  $t=15$ .

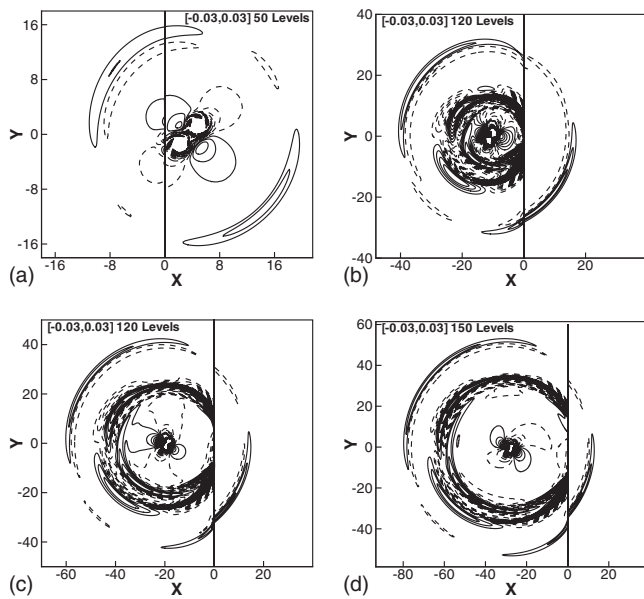


FIG. 12. The evolution of the sound pressure  $\Delta p = (p - p_s) / p_s$  of the shock interaction with two counter-rotating vortices.  $M_v = 0.25$ ,  $M_s = 1.2$ ,  $L = 20$ , and  $d = 4$ . (a)  $t = 15$ , (b)  $t = 30$ , (c)  $t = 40$ , (d)  $t = 50$ .

vortex pair and the separation distance between the two vortices are both 4. The angle  $\alpha$  is  $45^\circ$ . We observe that the precursor has two parts: the front and the peak. They are generated by two different processes. The front is the transmitted sound wave that is generated by the process of vortex coupling. The peak is generated by the interaction of the shock wave and the vortex pair. Because the initial vortex pair is close to the shock wave, as the sound wave generated by the vortex coupling impinges on the incident shock wave, the precursor is generated by the interaction of the incident shock wave and the vortex pair. As a result, the transmitted sound wave merges together with the precursor and becomes the front of the precursor.

As the initial distance  $L$  increases, the vortices undergo the coupling process while they are moving toward the shock wave. This coupling process generates sound waves which radiate outward. As a result, the sound wave generated by the vortex coupling will be separated from the sound wave generated by the shock interaction with the coupling vortices. Figure 12 is the evolution of the sound pressure of the shock interaction with two counter-rotating vortices. In this case, the strength of the shock wave and vortices and the separation distance between the two vortices are the same as in the case above, namely,  $M_s = 1.2$ ,  $M_v = 0.25$ , and  $d = 4$ . The initial distance is  $L = 20$ , which is much larger than in the case above. As can be seen from Fig. 12(a), the sound waves generated by the vortex coupling reach the shock wave much earlier than the vortices do. These sound waves interact with the shock wave before the vortices reach the shock wave. The transmitted sound waves propagate in the downstream of the shock wave. The shock wave is not deformed by the shock-sound interaction. As the vortices pass through the shock wave, new sound waves are generated by the shock vortex interaction. Figure 13 is the distribution of the sound pressure generated by the shock interaction with two

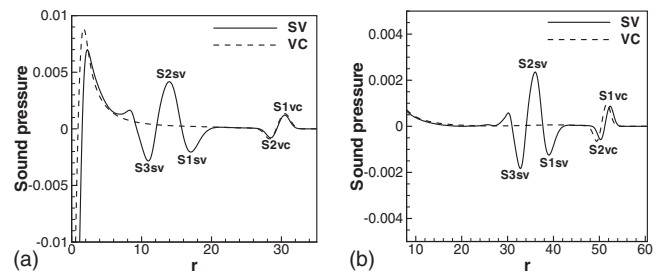


FIG. 13. The distribution of the sound pressure  $\Delta p = (p - p_s) / p_s$  generated by the shock interaction with two counter-rotating vortices and a comparison with that of free vortex coupling along the line from the middle of two vortices to the point of the maximum value of the first sound wave in the positive  $y$  plane.  $M_v = 0.25$ ,  $M_s = 1.2$ ,  $L = 20$ , and  $d = 4$ . Solid lines represent the sound pressure generated by the shock interaction with two counter-rotating vortices (SV). Dashed lines represent the sound wave generated by free vortex coupling (VC). (a)  $t = 30$ , (b)  $t = 50$ .

counter-rotating vortices and a comparison with that of free vortex coupling along the line from the middle of two vortices to the point of the maximum of the first sound pressure in the positive  $y$  plane.  $S1_{VC}$  and  $S2_{VC}$  represent the first and the second sound waves generated by the vortex coupling, respectively.  $S1_{SV}$ ,  $S2_{SV}$ , and  $S3_{SV}$  represent the first, the second, and the third sound waves generated by the shock interaction with the coupling vortex pair, respectively. At  $t = 30$ , the distance between the sounds  $S2_{VC}$  and  $S1_{SV}$  is approximately 10. The sound generated by the vortex coupling is much weaker than the sound generated by the shock vortex pair interaction. Hence, for this vortex with modest strength, the shock vortex pair interaction dominates the sound generation.

As the strength of the vortex increases, there are more sound waves generated by the vortex coupling, and the process of vortex coupling plays a more important role in the sound generation. Figure 14 is the evolution of the sound

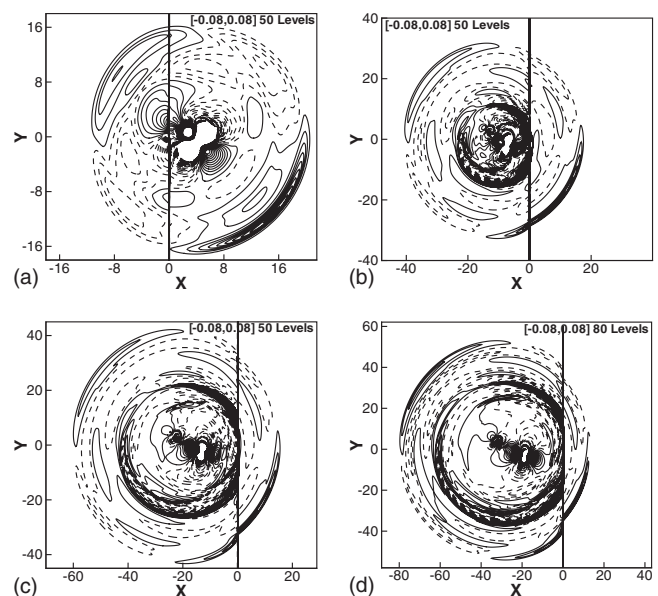


FIG. 14. The evolution of the sound pressure  $\Delta p = (p - p_s) / p_s$  of the shock interaction with two counter-rotating vortices.  $M_v = 0.8$ ,  $M_s = 1.2$ ,  $L = 20$ , and  $d = 4$ . (a)  $t = 15$ , (b)  $t = 30$ , (c)  $t = 40$ , (d)  $t = 50$ .



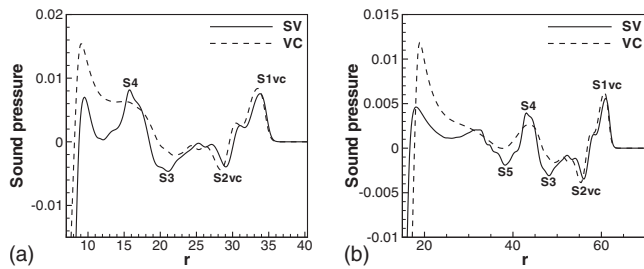


FIG. 15. The distribution of the sound pressure  $\Delta p = (p - p_s) / p_s$  along the line from the middle of two vortices to the point of the maximum value of the first sound wave in the positive  $y$  plane for the shock interaction with a vortex pair and a comparison with that of free vortex coupling.  $M_v = 0.8$ ,  $M_s = 1.2$ ,  $L = 20$ , and  $d = 4$ . Solid lines represent the sound pressure generated by shock vortex interaction (SV). Dashed lines represent the sound wave generated by free vortex coupling (VC). (a)  $t = 30$ , (b)  $t = 50$ .

pressure in the shock interaction with two counter-rotating vortices at  $M_s = 1.2$ ,  $M_v = 0.8$ , and  $L = 20$ . Figure 15 is the distribution of sound pressure generated by the shock interaction with two counter-rotating vortices and a comparison with that of free vortex coupling along the direction of  $45^\circ$ . There are two differences between this case and the case above. First, the sound wave generated by the vortex coupling is much stronger. Second, there is still the merging of the two processes of sound wave generation by vortex coupling and by shock vortex pair interaction.  $S1_{VC}$  and  $S2_{VC}$  are the first and second sound waves generated by the vortex coupling. They are the strongest sound waves.  $S_3$ ,  $S_4$ , and  $S_5$  contain the combination of the sound waves generated by vortex coupling and by shock vortex pair interaction.

If the initial distance between the shock wave and the vortex pair becomes larger, the vortex pair will gradually develop into two vortex dipoles due to the vortex coupling effect. The shock vortex pair interaction then becomes the interaction between the shock and two vortex dipoles.

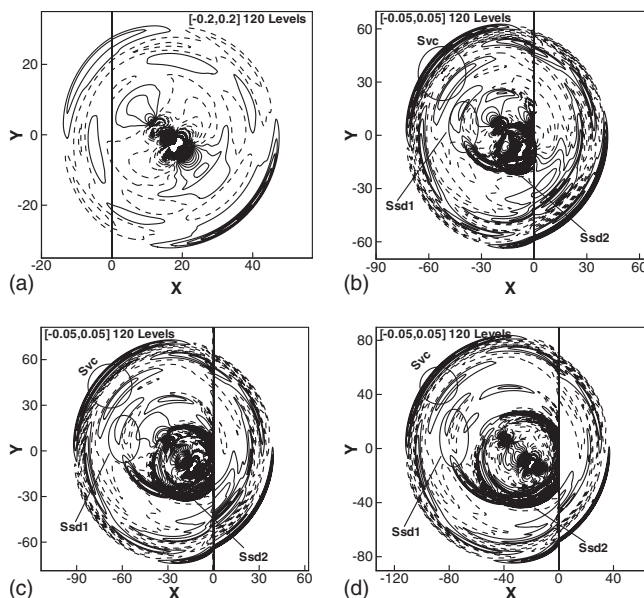


FIG. 16. The evolution of the sound pressure  $\Delta p = (p - p_s) / p_s$  of the shock interaction with two counter-rotating vortices.  $M_v = 0.8$ ,  $M_s = 1.2$ ,  $L = 50$ , and  $d = 4$ . (a)  $t = 30$ , (b)  $t = 60$ , (c)  $t = 70$ , (d)  $t = 80$ .

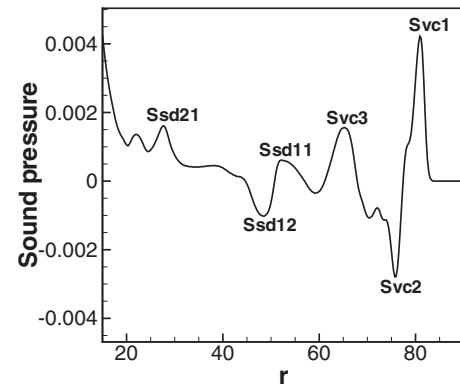


FIG. 17. The distribution of the sound pressure  $\Delta p = (p - p_s) / p_s$  along the line from the middle of two vortices to the point of the maximum value of the first sound wave in the positive  $y$  plane for the shock vortex pair interaction.  $M_v = 0.8$ ,  $M_s = 1.2$ ,  $L = 50$ ,  $d = 4$ , and  $t = 80$ .

Figure 16 contains the evolution of the sound wave generated by the shock interaction with two counter-rotating vortices. The Mach number of the shock wave is  $M_s = 1.2$ . The strength of the vortex pair is  $M_v = 0.8$ . The initial distance between the shock and the vortex pair is  $L = 50$ . As can be seen from Fig. 16(a), there are two vorticity fields before the vortex pair reaches the shock wave. These are the two undeveloped vortex dipoles. Figures 16(b) and 16(c) show that the sound waves contain three different parts:  $S_{VC}$ ,  $S_{SD1}$ , and  $S_{SD2}$ .  $S_{VC}$  is the sound wave generated by the vortex coupling,  $S_{SD1}$  is the sound wave generated by the interaction between the shock and the first vortex dipole, and  $S_{SD2}$  is the sound wave generated by the interaction between the shock and the second vortex dipole. Figure 17 is the radial distribution of the sound pressure along the symmetry line.

#### IV. CONCLUDING REMARKS

The interaction between a shock wave and two counter-rotating vortices is simulated systematically through solving the two-dimensional, unsteady compressible Navier–Stokes equations using a fifth order WENO finite difference scheme. The mechanism of sound generation is examined. The result shows that there are two regimes of sound generation in the shock interaction with two counter-rotating vortices, representing the shock interaction with two isolated vortices and the shock interaction with coupled vortex pair, respectively.

In the shock interaction with two isolated vortices, the sound generated by the shock interaction with two counter-rotating vortices equals to the linear combination of the sound waves generated by the two interactions between the same shock wave and each vortex. This scenario happens for the interaction between a shock wave and a weak vortex pair or a vortex pair with a large separation distance.

If the counter-rotating vortices are strong or the separation distance is small, the two vortices undergo a coupling process, which can be dominant in the second regime of sound generation. The distance between the shock wave and the vortex pair is a key parameter for the combined process. If the initial distance between the vortex pair and the incident shock wave is small, the sound generation process by the coupling effect and that for shock vortex pair interaction



merge together. If the initial distance is large enough, the sound wave generated by the vortex coupling can be separated from the sound wave generated by the shock vortex interaction. In the case of weaker vortex pair, the sound wave generated by the shock vortex interaction is stronger than the sound wave generated by the vortex coupling, and it dominates the sound wave in the shock vortex pair interaction. As the strength of the vortex pair increases, the sound wave generated by the vortex coupling becomes stronger and it finally dominates the sound wave in the shock vortex pair interaction.

If the initial distance between the vortex pair and incident shock wave is large enough, the process of vortex coupling is totally separated from the shock vortex interaction. The vortex pair undergoes a free evolution of coupling. As a result, two vortex dipoles are formed. The shock vortex pair interaction develops into an interaction between the shock wave and two vortex dipoles.

The sound wave generated by the shock vortex dipole interaction is similar to that of shock and vortex pair interaction. Two sound waves are generated in the interaction of a shock wave and a vortex dipole.

## ACKNOWLEDGMENTS

The research by Shuhai Zhang is supported by Chinese National Natural Science Foundation Grant Nos. 10572146 and 10772193 and 973 Program No. 2009CB724104. The research by Yong-Tao Zhang is partially supported by NSF Grant No. DMS-0810413 and Oak Ridge Associated Universities (ORAU) Ralph E. Powe Junior Faculty Enhancement Award. The research by Chi-Wang Shu is partially supported by NSF Grant Nos. DMS-0510345 and DMS-0809086 and by ARO Grant No. W911NF-08-1-0520.

<sup>1</sup>M. A. Hollingsworth and E. J. Richards, "A schlieren study of the interaction between a vortex and a shock wave in a shock tube," British Aeronautical Research Council Report No. 17985, Fluid Motion Subcommittee 2323, 1955.

<sup>2</sup>D. S. Dosanjh and T. M. Weeks, "Interaction of a starting vortex as well as a vortex street with a traveling shock wave," *AIAA J.* **3**, 216 (1965).

<sup>3</sup>A. Naumann and E. Hermanns, "On the interaction between a shock wave and a vortex field," AGARD Conf. Proc. **131**, 23.1 (1973).

<sup>4</sup>H. S. Ribner, "The sound generated by interaction of a single vortex with a shock wave," University of Toronto, Institute of Aerospace Studies (UTIA) Report No. 61, 1959.

<sup>5</sup>H. S. Ribner, "Cylindrical sound wave generated by shock-vortex interaction," *AIAA J.* **23**, 1708 (1985).

<sup>6</sup>D. S. Dosanjh and T. M. Weeks, "Sound generation by shock-vortex interaction," *AIAA J.* **5**, 660 (1967).

<sup>7</sup>L. Ting, "Transmission of singularities through a shock wave and the sound generation," *Phys. Fluids* **17**, 1518 (1974).

<sup>8</sup>L. Guichard, L. Vervisch, and P. Domingo, "Two-dimensional weak shock-vortex interaction in a mixing zone," *AIAA J.* **33**, 1797 (1995).

<sup>9</sup>J. L. Ellzey, M. R. Henneke, J. M. Picone, and E. S. Oran, "The interaction of a shock with a vortex: Shock distortion and the production of acoustic waves," *Phys. Fluids* **7**, 172 (1995).

<sup>10</sup>J. L. Ellzey and M. R. Henneke, "The shock-vortex interaction: The origins of the acoustic wave," *Fluid Dyn. Res.* **21**, 171 (1997).

<sup>11</sup>J. L. Ellzey and M. R. Henneke, "The acoustic wave from a shock-vortex interaction: Comparison between theory and computation," *Fluid Dyn. Res.* **27**, 53 (2000).

<sup>12</sup>O. Inoue and Y. Hattori, "Sound generation by shock-vortex interactions," *J. Fluid Mech.* **380**, 81 (1999).

<sup>13</sup>S. Zhang, Y.-T. Zhang, and C.-W. Shu, "Multistage interaction of a shock wave and a strong vortex," *Phys. Fluids* **17**, 116101 (2005).

<sup>14</sup>T. A. Manning, "A numerical investigation of sound generation in supersonic jet screech," Ph.D. thesis, Stanford University, 1999.

<sup>15</sup>C. C. M. Lui, "A numerical investigation of shock-associated noise," Ph.D. thesis, Stanford University, 2003.

<sup>16</sup>P. K. Ray, "Sound generated by instability wave/shock-cell interaction in supersonic jets," Ph.D. thesis, Stanford University, 2006.

<sup>17</sup>O. Inoue, T. Takahashi, and N. Hatakeyama, "Separation of reflected shock waves due to secondary interaction with vortices: Another mechanism of sound generation," *Phys. Fluids* **14**, 3733 (2002).

<sup>18</sup>S. Pirozzoli, F. Grasso, and A. D'Andrea, "Interaction of a shock wave with two counter-rotating vortices: Shock dynamics and sound production," *Phys. Fluids* **13**, 3460 (2001).

<sup>19</sup>S. Zhang, Y.-T. Zhang, and C.-W. Shu, "Interaction of an oblique shock wave with a pair of parallel vortices: Shock dynamics and mechanism of sound generation," *Phys. Fluids* **18**, 126101 (2006).

<sup>20</sup>G.-S. Jiang and C.-W. Shu, "Efficient implementation of weighted ENO schemes," *J. Comput. Phys.* **126**, 202 (1996).

<sup>21</sup>F. Grasso and S. Pirozzoli, "Simulations and analysis of the coupling process of compressible vortex pair: Free evolution and shock induced coupling," *Phys. Fluids* **13**, 1343 (2001).

<sup>22</sup>M. R. Schmidt, M. Beckers, A. H. Nielsen, J. J. Rasmussen, and G. J. F. van Heijst, "On the interaction between two oppositely signed, shielded, monopolar vortices," *Phys. Fluids* **10**, 3099 (1998).